



1 A new conceptual framework for assessing the state of the Baltic Sea

2 Urmas Raudsepp¹, Ilja Maljutenko¹, Priidik Lagemaa¹, Karina von Schuckmann²

3 ¹ Department of Marine Systems, Tallinn University of Technology, Tallinn, 12618, Estonia

4 ² Mercator Ocean international, 2 Av. de l'Aérodrome de Montaudran, 31400 Toulouse

5 *Correspondence to:* Ilja Maljutenko (ilja.maljutenko@taltech.ee)

6 Abstract.

7 A new conceptual framework for the assessment of the physical state of the general natural water basin was introduced and
8 then tested for the Baltic Sea. The model includes the analysis of mutual variability of ocean heat content (OHC), freshwater
9 content (FWC), subsurface temperature and salinity, atmospheric forcing functions along with salt transport across the open
10 boundaries as well as river runoff. The random forest model was used as the main analyses tool to highlight statistical
11 dependencies between state variables and potential forcing factors. Results show a distinct ocean warming trend in the Baltic
12 Sea over a 30-year period, which covaried at interannual scale with air temperature at 2-meter height, evaporation and wind
13 stress magnitude. Interannual changes of FWC were explained by large volume saline water inflows, net precipitation and
14 zonal wind stress. This framework offers a new perspective of the potential impact of a shallowing mixed layer depth,
15 resulting from sustained sensible heat flux changes at the air-sea interface, on salt export and the overall reduction of FWC in
16 the Baltic Sea. The study brought up that interannual variations of temperature and salinity within the vertically extended
17 halocline layer are major contributors to the OHC and FWC in the Baltic Sea.

18
19 **Short Summary.** In the last three decades, the Baltic Sea has experienced an increase in temperature and salinity. This trend
20 aligns with the broader pattern of atmospheric warming. The significant warming and the yearly fluctuations in the ocean's
21 heat content in the Baltic Sea are largely explained by subsurface temperature variations in the upper 100-meter layer, which
22 includes the seasonal thermocline and the permanent halocline. These fluctuations are influenced by factors such as air
23 temperature, evaporation, and the magnitude of wind stress. The changes in the sea's liquid freshwater content are primarily
24 driven by salinity shifts within the halocline layer, which extends vertically from 40 to 120 meters depth. However, salinity
25 changes in the upper layer play a minor role in the yearly variability of the freshwater content. The inflow of saline water,
26 overall precipitation, and zonal wind stress are the principal factors affecting the freshwater content changes in the Baltic
27 Sea.

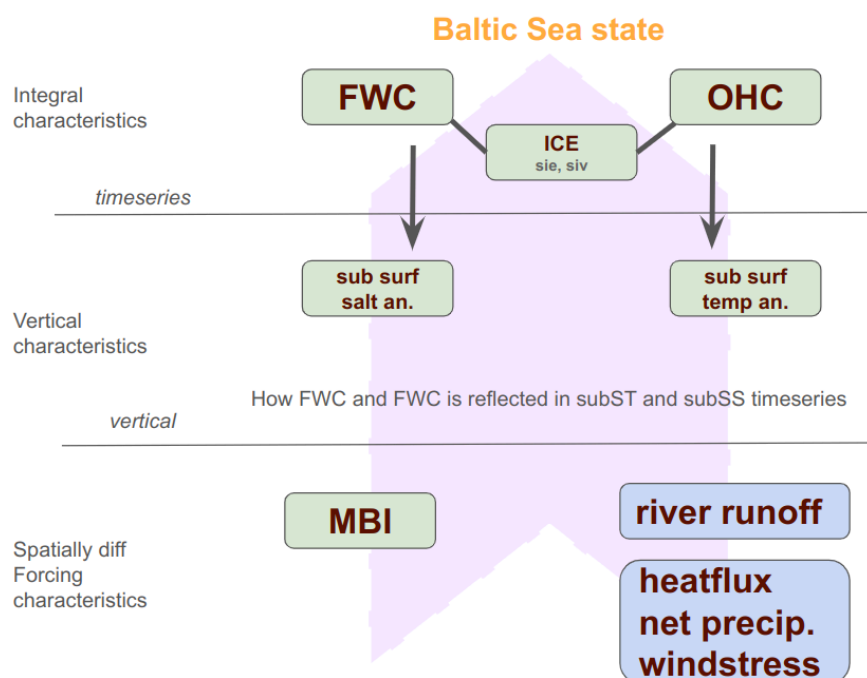


29 1 Introduction

30 Amidst global warming, increased air temperatures have led to higher ocean water temperatures and the melt of land-based
31 ice (IPCC, 2021). The former has caused a rise in Ocean Heat Content (OHC), while the latter has introduced significant
32 amounts of freshwater into the ocean, contributing to the rise in global sea levels. Most recently in 2023, there has been an
33 exceptional increase in global sea surface temperature (McGrath et al., 2024), and OHC reached unprecedented levels
34 (Cheng et al., 2024). Trends in Fresh Water Content (FWC) are not as consistent globally as those of OHC (Boyer et al.,
35 2007), although the rise in global sea level is widely acknowledged (Frederikse et al., 2020). Salinity patterns differ across
36 various ocean regions of the world (Skirris et al., 2014), with the North Atlantic–North Pacific salinity contrast increasing by
37 $5.9\% \pm 0.6\%$ since 1965 (Lu et al., 2024). At a regional scale in the Baltic Sea, FWC has shown a significant downward
38 trend over the last 30 years (Raudsepp et al., 2023).

39 The analysis of the physical state of natural water basins typically focuses on the evolution and spatial distribution of
40 temperature and salinity and corresponding uncertainty estimations (Lindstroem et al. 2012), which are essential ocean
41 variables (EOV). These variables are four dimensional and therefore provide spatially and temporarily resolved description
42 of the state of the water body. Meanwhile, OHC and FWC are vital integral characteristics of the ocean, indicative of a water
43 body's energy and mass, respectively. While OHC is a well-established indicator in ocean and climate research, its
44 counterpart, ocean FWC, has received less attention.

45 We propose the following conceptual model, which merges the analysis of temperature and salinity with their integral
46 counterparts OHC and FWC (Fig. 1). The initial phase entails determination of a water body, with boundaries that are either
47 geographical or arbitrarily set, and temporal resolution of the assessment of the physical state. The first stage consists of
48 calculating the time series of OHC and FWC of the whole water body under consideration. In basins covered partially by sea
49 ice, the annual mean ice extent (MIE) is deemed an important integral characteristic. These time series provide general
50 information on the evolution of the sea state. In the second stage, temporal changes of horizontally averaged vertical
51 distribution of temperature for OHC and salinity for FWC are examined. This enables us to determine which depth range of
52 subsurface temperature and salinity contribute the most to the variations of OHC and FWC. However, we refrain from
53 attributing any causal links between the changes and the driving forces. Still, the vertical profiles of salinity and temperature
54 provide clues about which forcing factors might be responsible for the variations in FWC and OHC. The third stage is
55 analyzing the forcing functions and integral state characteristics together, which enables identifying cause-and-effect
56 relationships. For this purpose, a suitable machine learning model is used. Implementing this approach can reveal a general
57 pattern in the temporal evolution of the physical state of the water body in question. An indicator-based framework relevant
58 to policy can enable the monitoring of changes in the Baltic Sea's state. It is not designed to offer an exhaustive dynamical
59 analysis, but rather to provide a scientifically robust and accessible framework. This information could serve as a valuable
60 resource for decision-makers and policymakers, while highlighting at the same time areas where detailed research on the
61 system's dynamics is needed.



62

63 **Figure 1:** Conceptual Scheme of the Baltic Sea State parameters.

64 This study evaluates a conceptual model for the Baltic Sea using annual mean values of ocean heat content (OHC),
 65 freshwater content (FWC), temperature, salinity, and a selection of forcing functions. The Baltic Sea is recognized for its
 66 spatially pronounced heterogeneous structure. Its various subregions may exhibit distinct temporal variations in key state
 67 variables and overall dynamics, making it a complex environment for testing the conceptual model. The Baltic Sea, a
 68 shallow marginal sea in northeastern Europe, is characterized by its hydrographic fields and sea ice conditions (Leppäranta
 69 and Myrberg, 2009). Salinity levels are affected by saline water inflows from the North Sea through the Danish straits,
 70 riverine freshwater inputs, and net precipitation (Lehmann et al., 2022). Major Baltic Inflows, which introduce saline and
 71 oxygen-rich water, are sporadic and unpredictable (Mohrholz, 2018). Temperature fields are influenced by the heat exchange
 72 with the atmosphere. The residence time of the Baltic Sea's water is several decades long (Meier et al., 2022). The vertical
 73 salinity stratification is defined by the halocline's depth, featuring a well-mixed surface layer and a slightly stratified layer
 74 beneath. Water temperature plays a crucial role in forming secondary stratification related to the temperature of the upper
 75 mixed layer. Seasonal temperature cycles lead to partial freezing of the Baltic Sea in winter. Changes in sea ice extent over
 76 time are a vital indicator of climate change for the area. A reduction in maximum ice extent impacts the sea's vertical
 77 stratification and the seasonal trends in ocean heat and freshwater content (Raudsepp et al., 2022; 2023). Despite global
 78 warming, there has not been a significant increase in the Baltic Sea's relative sea level (Ranasinghe et al., 2021) , which
 79 instead shows a strong seasonal cycle.



80 **2 Data and methods**

81 **Table 1:** Product Table

Product ref. no.	Product ID & type	Data access	Documentation
1	BALTICSEA_MULTIYEAR_PHY_003_011; Numerical models	EU Copernicus Marine Service Product (2023);	Quality Information Document (QUID): Panteleit et al. (2023); Product User Manual (PUM): Ringgaard et al. (2024)
2	ERA5; Numerical models	Copernicus Climate Change Service (2023)	Product reference: Hersbach et al., 2023 Journal article: Hersbach et al., 2020
3	E-HYPE; Numerical models	SMHI	Donnelly et al., 2016

82 **2.1 Oceanographic and atmospheric data**

83 The Baltic Sea physics reanalysis multi-year product (BAL-MYP; Table 1 product reference 1) is derived from the ocean
84 model NEMO v4.0 (Gurvan et al., 2019). It assimilates satellite observations of sea surface temperature (SST) (EU
85 Copernicus Marine Service Product, 2022) and in-situ temperature and salinity profiles from the ICES database (ICES Bottle
86 and low-resolution CTD dataset, 2022). The model data is provided on a grid with a horizontal resolution of 1 nautical mile,
87 including 56 vertical layers, covering the entire Baltic Sea and the transition zone to the North Sea. The dataset covers the
88 period from 1993 to 2023, with the model setup detailed in the Product User Manual (PUM, Ringgaard et al., 2024).

89 The BAL-MYP has been extensively validated, as documented in the Quality Information Document (QuID; Panteleit et al.,
90 2023), focusing on the period from 1st January 1993 to 31st December 2018. Additionally, the BAL-MYP data were
91 evaluated using a clustering method with the K-means algorithm (Raudsepp and Maljutenko, 2022), which provided insights
92 into the reanalysis accuracy by categorising errors (Lindenthal et al., 2023). Fifty-seven percent of the data are clustered with
93 a bias of $dS = -0.40$ g/kg and $dT = -0.02$ °C, encompassing 57% of all data points with RMSE $S = 0.92$ g/kg and $T = 0.54$ °C.
94 These points are distributed throughout the Baltic Sea. Clusters with high positive and negative temperature biases account
95 for 11% and 8% of total points, respectively, with marginal salinity biases and relatively even spatial distributions across the
96 Baltic Sea. Twenty-six percent of the points have low temperature but high salinity errors, both negative and positive,
97 predominantly located in the southwestern Baltic Sea, indicating occasional underestimation or overestimation of the
98 inflow/outflow salinity.

99 The daily Ocean Heat Content (OHC) has been computed for each model grid cell from reanalysis (product reference 1),
100 following the methodology of Meyssignac et al. (2019). The Freshwater Content (FWC) was determined at each grid point



and day as per Boyer et al. (2007), with a more detailed description of the calculation procedure available in Raudsepp et al. (2023). The OHC and FWC were calculated by spatially integrating the gridded FWC over the Baltic Sea, and then the annual mean OHC and FWC values were derived from these daily values.

Atmospheric data were obtained from the ERA5 reanalysis (Table 1 product ref 2) for the period 1993–2023. The parameters included 2-meter air temperature, total precipitation, evaporation, wind stress magnitude, and the x- and y-components of wind stress, along with total cloud cover and surface net solar radiation. The time series for the annual mean values of these atmospheric parameters were computed as horizontal averages across the Baltic Sea region.

2.2 Random Forest

Random Forest (RF) is an ensemble learning method predominantly used for classification and regression tasks (Breiman, 2001). It functions by building multiple decision trees during the training phase and outputs the class that is the mode of the classes (classification) or the mean prediction (regression) of the individual trees. This method enhances accuracy and helps prevent overfitting, thus making it resilient to noise in the dataset. RF proves to be highly effective in analyzing complex interactions between variables, such as the relationships between marine state variables and atmospheric parameters. Its effectiveness is due to its capability to manage high-dimensional data and its resistance to outliers and noise, which are prevalent in environmental datasets. Additionally, RF is adept at detecting nonlinear relationships between predictor variables (atmospheric parameters) and response variables (marine state variables), which linear models often overlook.

In the context of an RF model, feature importance is a technique that identifies the most influential input features (variables) in predicting the output variable. The importance of each feature is determined by the decrease in model accuracy when the data for that feature is permuted, while all other features remain unchanged. If permuting a feature's values significantly increases the model's error, that feature is deemed crucial for the model's predictions. This approach aids in discerning the contribution of each feature to the model's decision-making process and in identifying key atmospheric parameters that significantly impact marine state variables. A positive value for a feature implies that permuting that predictor variable's values raises the model's prediction error, indicating the variable's importance for the model's predictive accuracy. A higher positive value suggests greater reliance on that variable by the model.

In this study utilising Random Forest (RF), we trained an ensemble of 150 individual models, each comprising 100 decision trees. This technique captures the variability in feature importance across different model training iterations, influenced by the random selection of features and data points in each tree. We employed MATLAB's TreeBagger function to assess the feature importance of atmospheric predictors on marine state variables. The 'OOBPermutedPredictorDeltaError' method, a robust metric from MATLAB's TreeBagger, quantifies each predictor's importance via the out-of-bag (OOB) prediction error. This involves permuting each variable's values across OOB observations for each tree. The resulting change in prediction error from these permutations is calculated for each tree. These measures are averaged across all trees and normalised by the standard deviation of the changes, providing a standardised score that highlights the variables with the most significant



133 impact on predictive accuracy. Averaging the feature importance scores across all 150 models minimises the noise and
134 variability from any single model's training, offering a more consistent and dependable indication of each atmospheric
135 parameter's contribution to predicting marine state variables.

136 **3 Results**

137 Both OHC and FWC display a statistically significant linear trend, as shown in Figure 2. Using a z-score time series allows
138 for the comparison of trends and data distributions without the influence of their units. OHC shows an increasing trend of
139 0.089 ± 0.025 , while FWC exhibits a decreasing trend of -0.092 ± 0.023 , both comparable in magnitude (Table 2). The
140 corresponding absolute values are 0.34 ± 0.095 W/m² for OHC and -36.99 ± 9.20 km³ for FWC (Table 2). Between 1993 and
141 2003, OHC and FWC varied similarly, both rising and falling concurrently (blue dots in Fig. 2). After this period, their
142 patterns diverged (yellow and red dots in Fig. 2). Interannual variations of the annual mean sea ice extent and OHC are
143 strongly correlated but in opposite phases. Among the forcing functions, the 2-metre air temperature shows a distinct positive
144 trend (Fig. 2), albeit weaker than the trends of OHC and FWC (Table 2). The air temperature over the Baltic Sea area has
145 risen at a rate of 0.074 ± 0.031 °C/year (Table 2). Surface net solar radiation has a weaker but still significant positive trend of
146 0.058 ± 0.035 , and the evaporation time series shows a negative trend of -0.041 ± 0.039 (Fig. 2, Table 2). Other atmospheric
147 variables did not exhibit statistically significant trends (Fig. 2). Correlation coefficients among various atmospheric datasets
148 were generally low (Table 3). The two highest correlation coefficients, 0.76 and 0.73, are between wind stress magnitude and
149 its zonal component, indicating a predominance of westerly airflow over the Baltic Sea, and between 2-metre air temperature
150 and surface net solar radiation, respectively. The low correlations suggest a weak statistical relationship between the annual
151 mean atmospheric parameters, supporting the inclusion of all forcing functions in the RF model.

152 **Table 2.** Linear annual trend values of z-scored time series (trend*), standard deviation (STD), linear trend value (trend) and
153 mean value (mean) of original time series. *OHC*: ocean heat content, *FWC*: fresh water content, *T2*: 2 metre temperature, *TP*:
154 total precipitation, *EVAP*: evaporation, *Wstr*: windstress, *WUstr*: windstress u component, *WVstr*: windstress v component,
155 *TCC*: total cloud cover, *SSR*: surface net solar radiation, *RNF*: river runoff.

Variable:	OHC	FWC	T2	TP	EVAP	Wstr	WUstr	WVstr	TCC	SSR	RNF
Unit	MJ/m ²	km ³	°C	m/y	m/y	N/m ²	N/m ²	N/m ²	l	W/m ²	m ³ /s
trend*:	0.089 ± 0.025	-0.092 ± 0.023	0.074 ± 0.031	0.032 ± 0.04	-0.041 ± 0.039	-0.0016 ± 0.0418	0.013 ± 0.041	0.015 ± 0.041	-0.0077 ± 0.0417	0.058 ± 0.035	0.0073 ± 0.0417
STD:	122.02	402.00	0.73	0.071	0.041	0.0056	0.0100	0.0072	0.0226	3.16	1,687.92
trend:	0.344 (W/m ²)	-36.987	0.054	0.0023	-0.0016	-8.85×10^{-6}	1.32×10^{-4}	1.05×10^{-4}	-1.75×10^{-4}	0.18	12.31
mean:	60.20	-63.73	7.65	0.73	-0.55	0.0999	0.0244	0.0138	0.6493	113.92	17,807.77



Table 3. Correlations coefficients (lower triangle) and StandardErrors (Gnambs, 2023) (upper triangle) of atmospheric parameters. Correlation coefficients which pass two-tailed t-test at 95% confidence are in bold. *OHC*: ocean heat content, *FWC*: fresh water content, *T2*: 2 metre temperature, *TP*: total precipitation, *EVAP*: evaporation, *Wstr*: wind stress magnitude, *WUstr*: wind stress u component, *WVstr*: wind stress v component, *TCC*: total cloud cover, *SSR*: surface net solar radiation.

	<i>T2</i>	<i>TP</i>	<i>EVAP</i>	<i>Wstr</i>	<i>WUstr</i>	<i>WVstr</i>	<i>TCC</i>	<i>SSR</i>
<i>T2</i>		0.19	0.17	0.17	0.15	0.14	0.15	0.09
<i>TP</i>	0.12		0.18	0.17	0.18	0.18	0.13	0.17
<i>EVAP</i>	-0.28	-0.18		0.19	0.18	0.16	0.19	0.15
<i>Wstr</i>	0.31	0.35	-0.10		0.08	0.15	0.18	0.19
<i>WUstr</i>	0.47	0.25	0.16	0.76		0.15	0.16	0.18
<i>WVstr</i>	0.48	0.16	0.37	0.43	0.43		0.19	0.19
<i>TCC</i>	-0.43	0.58	-0.04	-0.20	-0.42	-0.13		0.09
<i>SSR</i>	0.73	-0.31	-0.43	0.07	0.18	0.11	-0.73	

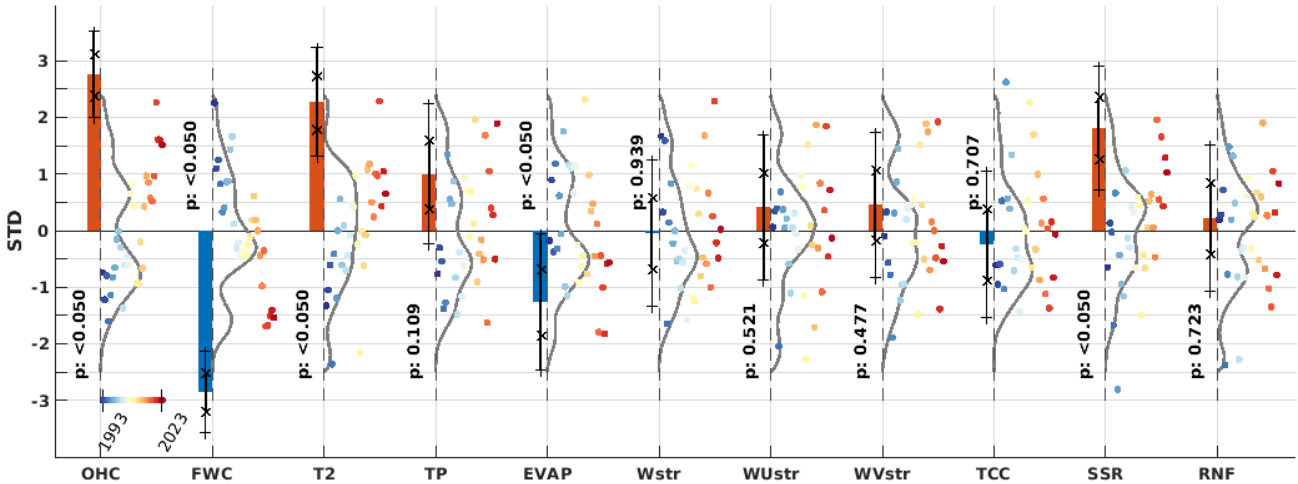


Figure 2: Trend analysis and probability distribution functions (PDFs) of the annual time series of standardized (*z-scores) Baltic Sea state and meteorological parameters. To the left of the dashed line, the period-normalized annual trend values (multiplied by the period length in years i.e. 30) are displayed with corresponding p-values (95% confidence level), along with whiskers representing ± 1 standard error (x ticks) and the 95% uncertainty range (+ ticks). On the right side, PDFs are shown for the standardized time series, represented by colored dots. For each dashed axis following variable stands *OHC*: ocean heat content, *FWC*: fresh water content, *T2*: 2 metre temperature, *TP*: total precipitation, *EVAP*: evaporation, *Wstr*: windstress, *WU/WVstr*;; windstress u and v component, *TCC*: total cloud cover, *SSR*: surface net solar radiation, *RNF*: river runoff.

In analyzing OHC variations, we use a RF model. This model employs horizontally averaged annual temperature values at each depth level, derived from the depth levels of a multi-year product (Table 1 product ref 1), as input features. The RF



172 model finely replicates the annual OHC time series (Fig 3a), with high correlation coefficient (0.986) and a RMSD of the
173 standardized time series at 0.0016. However, it did not capture the extreme OHC event in 2020 or the low OHC extreme in
174 1996 (Fig. 3). Feature importance is significant within a depth range of 10-80 meters (Fig. 3b), with two peaks at depths of
175 18 and 60 meters, aligning with the average depths of the seasonal thermocline and the permanent halocline, respectively.
176 This suggests that interannual OHC variations are mainly influenced by temperature changes within these layers. Subsurface
177 temperatures from 1993 to 2023 indicate warming trends of approximately 0.06 °C/year across all depths (CMS 2024a).
178 From 1993 to 1997, deep water temperatures remained relatively low (below 6 °C). Since 1998, deeper waters have warmed,
179 with temperatures above 7 °C occupying the layer below 100 meters since 2019. The water temperature below the halocline
180 has risen by about 2 °C since 1993, and the cold intermediate layer's temperature has also increased during the 1993-2023
181 period.

182 A similar method is employed to elucidate the inter-annual fluctuations of FWC, utilizing horizontally averaged salinity at
183 each depth level. The model's precision is slightly lower (Correlation: 0.973, RMSD of standardized time series: 0.004)
184 compared to that for OHC. The model consistently underperforms in predicting the FWC peaks, encompassing both the lows
185 and highs (Fig. 3c). The most notable features cover the depth range of 40-120 meters (Fig. 3d), coinciding with a halocline
186 layer and its vertical extensions to both shallower and deeper depth. The salinity levels at the bottom layer are of secondary
187 importance to the inter-annual variations of FWC in the Baltic Sea. The salinity in the top 25-meter stratum exerts a minimal
188 influence on FWC changes. The interannual variability of salinity in the upper stratum is minor relative to the deeper
189 stratum. The salinity gradient ascends steadily from zero at a depth of 25 meters to 0.04 g/kg annually at 70 meters (CMS
190 2024b). The most marked trend, 0.045 g/kg per annum, occurs within the expanded halocline layer extending from 70 to 150
191 meters. Notably, there is a slight dip in the salinity trend to 0.04 g/kg per annum between the depths of 150 and 220 meters.
192 While this reduction is slight, it indicates that salt influx into the expanded halocline layer is more significant than into the
193 deeper strata. A salinity trend of 0.05 g/kg annually is detected in the deepest stratum of the Baltic Sea.

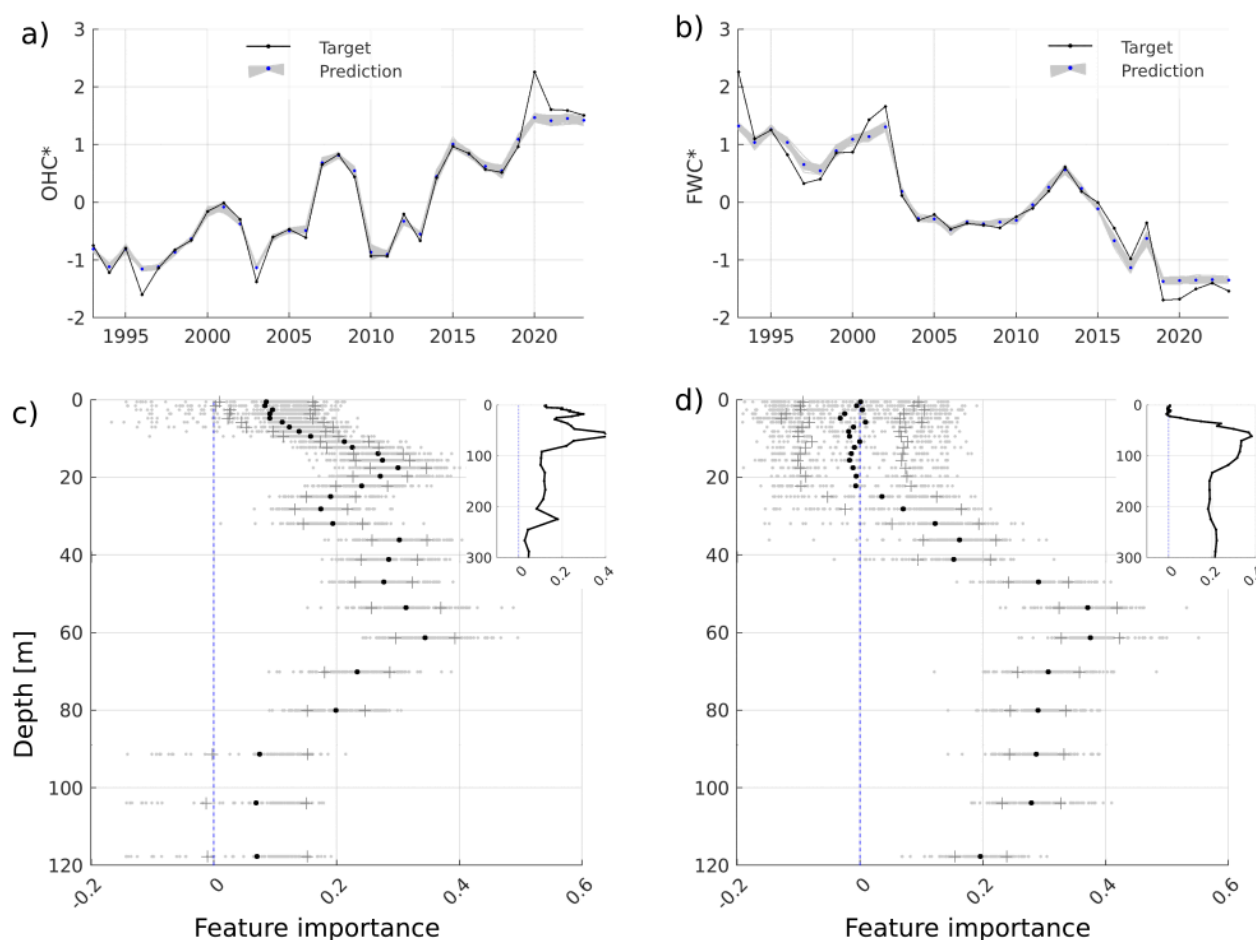


Figure 3: OHC* and FWC* ensemble predictions (ens. mean as blue dots) using the horizontal average salinity and temperature profiles (a), (b). The prediction features importance for each depth in the upper 120 m layer shown on c) and d) and for full depth range in the upper-right inset panels. All variables are z-scored.

Building a RF model targeting OHC and FWC functions with atmospheric forcing functions reveals the 2-meter air temperature as the most significant contributor (not shown). This correlation is physically plausible for OHC but less so for FWC. The 2-meter air temperature affects the air-sea heat exchange via the sensible heat flux component. To further explore the declining FWC trend, we examined interannual changes in the annual average upper mixed layer depth (MLD). In the Baltic Sea, MLD varies widely across different areas and seasons. A shallowing of MLD is observed in the Baltic Proper and to some extent in the Bothnian Sea, while a MLD deepening is noted in the Bothnian Bay, the Gulf of Finland, and the Gulf of Riga. Typically, the Baltic Sea's stratification is influenced by salinity, although a seasonal thermocline forms across the sea. In the northern and eastern basins, the dispersal of river water during spring and summer leads to the development of the



seasonal pycnocline. Conversely, in the southern Baltic Sea, the spread of river water is mostly restricted to the coastal areas, so the mixed layer is less affected by the seasonal halocline.

We performed test experiments with the RF model, incorporating the upper mixed layer (UML) as an additional feature. We determined the annual mean UML depth across the Baltic Sea and specifically for the Eastern Gotland Basin. The decline in the UML depth was more significant in the Eastern Gotland Basin compared to the entire Baltic Sea. The UML depth in the Eastern Gotland Basin decreased from 30 meters in 1993 to 22 meters in 2023. The MLD feature became more significant than the 2-meter temperature in explaining the FWC when we considered the UML depth in the Eastern Gotland Basin. However, the results were contentious when we applied the average UML depth for the entire Baltic Sea. An increase in the 2-meter temperature may cause a shallower mixed layer, potentially reducing the mixing between the surface freshwater layer and the denser saline layer beneath. Given the short residence time of surface layer water in the Baltic Sea, a shallower UML could result in less salt being transported out of the sea compared to a deeper UML.

By eliminating trends, we utilized RF models to identify the primary characteristics of the interannual fluctuations of OHC and FWC. The ensemble mean forecast of OHC effectively captures these interannual changes (Fig. 4a), evidenced by a correlation coefficient of 0.9012 and a RMSD of 0.3432. Factors such as 2-meter temperature, wind stress, and evaporation significantly influence the interannual variability of OHC (Fig. 4c). Additionally, total cloud cover and solar radiation have a minor impact on the shape of OHC.

In the FWC model, we incorporated bottom salinity from the Bornholm Basin as a supplementary feature. The direct calculation of salt transport from model data across a section at the Baltic Sea entrance is error-prone. Utilizing daily average cross-section velocities and salinities overlooks high-frequency fluctuations with considerable residual salt flux. The model's precision in predicting accurate salinity levels at the Baltic Sea's entrance is quite low. Time series of bottom salinity changes in the Arkona and Bornholm Basins facilitate the tracking of the intermittent nature of water inflow and outflow events. The Arkona Basin, being relatively shallow, is known for its dynamic nature regarding volume and salt transport. Here, bottom salinity reflects the salinity shifts caused by inflow and outflow variations at the Baltic Sea entrance. These variations mask the large volume inflows chiefly responsible for the Baltic Sea's salt influx, thus not significantly affecting the Arkona Basin's bottom salinity over time. Conversely, the Bornholm Basin's greater depth means its bottom salinity is less affected by the upper layer's varying salinity water movements. Hence, the Bornholm Basin's bottom salinity serves as a more accurate indicator of the Baltic Sea's salt influx. We also factored in the annual average river runoff (Table 1 product ref 3) into the Baltic Sea in our RF model.

The ensemble mean predictions of the FWC are marginally less precise, with a correlation coefficient of 0.8994 and a root mean square difference of 0.3624. Notable peaks in the FWC occurred in 1993, 2002, and 2013, each followed by a swift decline in subsequent years (Fig. 4b). The bottom salinity in the Bornholm Basin, serving as an indicator for salt flux into the Baltic Sea, along with total precipitation and the zonal wind component, are the primary factors influencing the FWC's

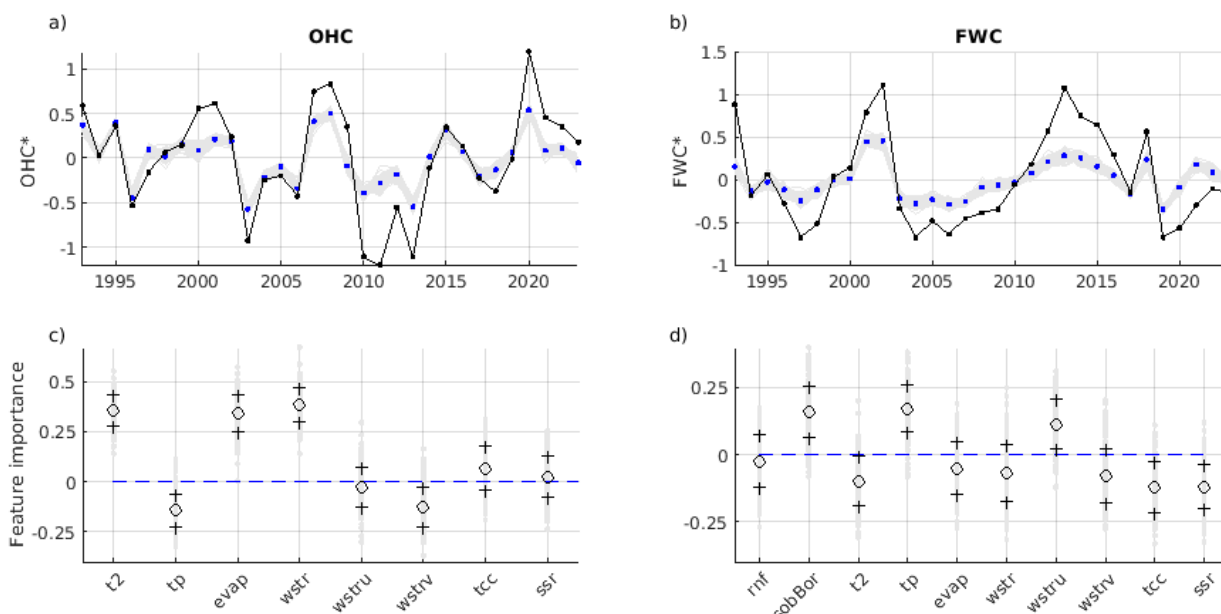


Figure 4: Time series of detrended OHC* (a) and FWC* (b) ensemble predictions (ens. mean as blue dots) using RF ensembles. Ensembles of corresponding models feature importances shown on (c) and (d) for OHC and FC respectively. All variables are z-scored. OHC: ocean heat content, FWC: fresh water content, T2: 2 metre temperature, TP: total precipitation, EVAP: evaporation, Wstr: windstress, WU/WVstr: windstress u and v component, TCC: total cloud cover, SSR: surface net solar radiation, RNF: river runoff, sobBor: bottom salinity in the deepest location of the Bornholm basin.

4. Discussion and Conclusions

We proposed a new conceptual framework where the Baltic Sea's state is defined by two main factors: OHC and FWC. We employed the RF model (Breiman, 2001) to link the forcing functions with the variability of OHC and FWC. Our analysis across the entire Baltic Sea reveals the direct impact of atmospheric forcing on ocean warming. Moreover, this framework provides new insights into the role of salt import/export in FWC's interannual variability, and draws on the basin-wide decline of FWC, elevating the potential role of a flattening MLD from long-term sensible flux change at the air-sea interface. Particularly, results reveal that the Baltic Sea has undergone substantial change over the past decade as evidenced by the increase in OHC over the last thirty years.



257 Simultaneously, there has been a reduction in FWC, suggesting an increase in seawater salinity. The analysis of average
258 subsurface temperature and salinity indicates that interannual variations in OHC and FWC are mainly influenced by
259 temperature shifts in both the seasonal thermocline and permanent halocline and changes in salinity within the permanent
260 halocline. This highlights the critical need for a comprehensive framework while reporting on the state of the Baltic Sea,
261 allowing for the evaluation of basin-wide conditions, including its trends, interannual variations, and extremes, as well as the
262 factors driving these changes. Using this approach could prove to be a valuable asset for the science-policy interface, aiding
263 in regional evaluations of the sea state. .

264 Previous studies have reported a positive trend in OHC and a negative trend in FWC (Raudsepp et al., 2022; 2023), along
265 with an inverse relationship between OHC and the maximum ice extent in the Baltic Sea (Raudsepp et al., 2022). The
266 increase in OHC has been attributed to the rising air temperature over the Baltic Sea, yet the decline in FWC remains largely
267 unexplained. Raudsepp et al. (2023) noted that neither salt transport to the Baltic Sea, net precipitation, nor total river runoff
268 accounted for the FWC's downward trend. Despite this, deepwater salinity in the central Baltic Sea has been increasing at a
269 rate of 0.2–0.25 g kg⁻¹ per decade (Lehmann et al., 2022). A basin-wide analysis linking FWC changes to atmospheric forces
270 revealed a correlation with air temperature, a connection that is physically tenuous, prompting further investigation into other
271 factors. This led to the hypothesis that the decreasing trend in the upper mixed layer thickness in the Baltic Sea might be
272 influencing FWC changes. Over the last three decades, there has been a noticeable reduction in the upper mixed layer depth.
273 While it is plausible to suggest a dynamic relationship between the shrinking mixed layer depth and the decrease in FWC,
274 verifying this hypothesis requires more research than what is covered in the present study.

275 Interannual variations of OHC are influenced by air temperature, evaporation, and wind stress magnitude over the Baltic Sea
276 (Fig. 4). When considering the lesser impact of total cloud cover and surface net solar radiation, it becomes clear that air-sea
277 heat exchange primarily drives OHC changes in the Baltic Sea. Notably, the annual mean OHC parallels the long-term trend
278 of winter OHC in the Baltic Sea's upper 50-m layer (Raudsepp et al., 2022), highlighting the influence of seasonal ice cover
279 on OHC fluctuations. In seas with seasonal ice cover, the characteristics of sea ice are crucial for determining the sea's
280 physical state. Typically, the maximum sea ice extent in the Baltic Sea indicates the severity of the winters (Uotila et al.,
281 2015). Sea ice is vital for temporarily storing ocean heat and freshwater, then releasing it back into the sea.

282 The interannual variations of FWC were associated with Major Baltic Inflows, overall precipitation, and zonal wind stress
283 (Fig. 4). Major Baltic Inflows inflows are crucial in shaping the hydrophysical conditions of the central Baltic Sea's deep
284 regions, significantly affecting marine ecology across various trophic levels (Bergen et al., 2018). Without Major Baltic
285 Inflows, the deeper layers of the central Baltic become oxygen-depleted, leading to the emergence of hydrogen sulphide (as
286 noted by Savchuk, 2018). Furthermore, increased water temperatures have hastened oxygen depletion, causing the hypoxic
287 areas to expand (Safonova et al., 2024). Consequently, the ongoing reduction in FWC and the rise in OHC signal a growth in
288 the hypoxic and anoxic zones within the Baltic Sea.



Meier and Kauker (2003) demonstrated that increasing westerly winds could hinder the outflow of freshwater from the Baltic Sea, leading to decreased salt transport into the sea. While several studies have underscored a correlation with river runoff (Kniebusch et al., 2019; Radtke et al., 2020; Lehmann et al., 2022), our research did not find this connection.

The OHC exhibits oscillations with a period of 5-7 years, reaching a high extreme in 2020 and a low extreme in 2011 (Fig. 4). The period from January to March 2020 was notably warm over the Northern Hemisphere (Schubert et al., 2022), which was evident in the Baltic Sea's winter OHC (Raudsepp et al., 2022). Additionally, the year 2020 was marked by an exceptionally high marine heatwave index (Bashiri et al., 2024) and a significant number of marine heatwave days (Lindenthal et al., 2023). Conversely, 2011 saw the greatest sea ice extent and volume of the past three decades (Raudsepp et al., 2022). Notably, high extremes in FWC, such as those in 2002 and 2013 (Fig. 4), precede Major Baltic Inflow events, whereas low extremes, such as those in 1997 and 2019, follow several years after these events.

Global warming, with its increased frequency and intensity of extreme events, has had widespread negative impacts on nature and significant socioeconomic repercussions (IPCC, 2021). Our methodology has highlighted the extremes of interannual variability in OHC and FWC. In our study, we utilized the RF model to investigate the relationships between changes in OHC and FWC and their potential drivers. Although the model pinpointed the primary factors, it failed to capture the extremes (Gnecco et al., 2024), as illustrated in Fig. 4a,b. RF models tend to underperform when extreme values are not well-represented in the training data, a common issue in ecological modeling and other practical applications (Fox et al., 2017). This can result in a bias where the model does not recognize or accurately predict rare but impactful events, such as extreme weather conditions, uncommon species occurrences, or anomalies in financial markets (Fox et al., 2017). Acknowledging this, we hypothesize that while primary forces set the stage for extreme events, these events themselves fall outside the scope of standard interannual variability and stem from a distinct combination of forces. Consequently, it is advantageous to analyze extreme events independently from typical interannual variations (Nontapa et al., 2020; Chen et al., 2021). To account for the variations in OHC and FWC, models other than RF, such as deep machine learning models, could be employed, especially if the temporal resolution is monthly (e.g., Barzandeh et al., 2024) or finer, ensuring a representative dataset is available. Advancing this methodology will further our comprehension of the causes behind extreme events, thereby improving our predictive abilities.

Data Availability

This study is based on public databases and the references are listed in Table 1.

Competing Interests

The authors declare that they have no conflict of interest.



320 Disclaimer

321 The Copernicus Marine Service offering is regularly updated to ensure it remains at the forefront of user requirements. In
322 this process, some products may undergo replacement or renaming, leading to the removal of certain product IDs from our
323 catalogue.

324 If you have any questions or require assistance regarding these modifications, please feel free to reach out to our user support
325 team for further guidance. They will be able to provide you with the necessary information to address your concerns and find
326 suitable alternatives, maintaining our commitment to delivering top-quality services.

327 References

- 328 Barzandeh, A., Maljutenko, I., Rikka, S., Lagemaa, Männik, A., P., Uiboupin, R., Raudsepp, U.: Sea surface circulation in
329 the Baltic Sea: decomposed components and pattern recognition. *Sci. Rep.*, 14, 18649,
330 <https://doi.org/10.1038/s41598-024-69463-8>, 2024
- 331 Bashiri, B., Barzandeh, A., Männik, A., Raudsepp, U.: Marine heatwaves' characteristics and assessment of their potential
332 drivers in the Baltic Sea over the last 42 years. *Sci. Rep.* (submitted), 2024
- 333 Bergen, B., Naumann, M., Herlemann, D.P.R., Gräwe, U., Labrenz, M., Jürgens, K.: Impact of a major inflow event on the
334 composition and distribution of bacterioplankton communities in the Baltic Sea. *Front. Mar. Sci.*, 5, 383,
335 <https://doi.org/10.3389/fmars.2018.00383>, 2018
- 336 Boyer, T., Levitus, S., Antonov, J., Locarnini, R., Mishonov, A., Garcia, H., Josey, S.A.: Changes in freshwater content in the
337 North Atlantic Ocean 1955–2006. *Geophys. Res. Lett.*, 34, L16603, <https://doi.org/10.1029/2007GL030126>, 2007
- 338 Breiman, L.: Random forests. *Mach. Learn.*, 45, 5–32, <https://doi.org/10.1023/A:1010933404324>, 2001
- 339 Chen, S., Ren, M., Sun, W.: Combining two-stage decomposition based machine learning methods for annual runoff
340 forecasting. *J. Hydrol.*, 603B, 126945, <https://doi.org/10.1016/j.jhydrol.2021.126945>, 2021
- 341 Cheng, L., von Schuckmann, K., Minière, A., Schmidt, G.A., Pan, Y.: Ocean heat content in 2023. *Nat. Rev. Earth Environ.*,
342 5, 232–234, <https://doi.org/10.1038/s43017-024-00539-9>, 2024
- 343 Copernicus Climate Change Service: ERA5 hourly data on single levels from 1940 to present. Copernicus Climate Change
344 Service (C3S) Climate Data Store (CDS), <https://doi.org/10.24381/cds.adbb2d47>, last access: 4 April 2024
- 345 CMS: Baltic Sea subsurface temperature trend from reanalysis. E.U. Copernicus Marine Service Information (CMEMS)
346 Marine Data Store (MDS), <https://doi.org/10.48670/moi-00208>, 2024a
- 347 CMS: Baltic Sea subsurface salinity trend from reanalysis. E.U. Copernicus Marine Service Information (CMEMS) Marine
348 Data Store (MDS), <https://doi.org/10.48670/moi-00207>, 2024b
- 349 Donnelly, C., Andersson, J.C., Arheimer, B.: Using flow signatures and catchment similarities to evaluate the E-HYPE
350 multi-basin model across Europe. *Hydrol. Sci. J.*, 61, 255–273, <https://doi.org/10.1080/02626667.2015.1027710>, 2016
- 351 EU Copernicus Marine Service Product: Baltic Sea - L3S Sea Surface Temperature Reprocessed. Mercator Ocean Int.,
352 <https://doi.org/10.48670/moi-00312>, 2022



- 353 EU Copernicus Marine Service Product: Baltic Sea physics reanalysis. Mercator Ocean Int.,
354 <https://doi.org/10.48670/moi-00013>, 2023.
- 355 Frederikse, T., Landerer, F., Caron, L., Adhikari, S., Parkes, D., Humphrey, V.W., Dangendorf, S., Wu, Y.-H.: The causes of
356 sea-level rise since 1900. *Nature*, 584, 393–397, <https://doi.org/10.1038/s41586-020-2591-3>, 2020.
- 357 Fox, E.W., Hill, R.A., Leibowitz, S.G., Olsen, A.R., Thornbrugh, D.J., Weber, M.H.: Assessing the accuracy and stability of
358 variable selection methods for random forest modeling in ecology. *Environ. Monit. Assess.*, 189, 316,
359 <https://doi.org/10.1007/s10661-017-6025-0>, 2017
- 360 Gnambs, T.: A brief note on the standard error of the Pearson correlation. *Collabra Psychol.*, 9, 1–7,
361 <https://doi.org/10.1525/collabra.87615>, 2023
- 362 Gnecco, N., Terefe, E.M., Engelke, S.: Extremal random forests. *J. Am. Stat. Assoc.*, 1–14,
363 <https://doi.org/10.1080/01621459.2023.2300522>, 2024
- 364 EOV: Essential ocean variables. EOV, <https://goosocean.org/what-we-do/framework/essential-ocean-variables/>, accessed on
365 4 September 2024
- 366 Gurvan, M., Bourdallé-Badie, R., Chanut, J., et al.: NEMO ocean engine. Notes du Pôle de modélisation de l'Institut
367 Pierre-Simon Laplace (IPSL), v4.0, Number 27, <https://doi.org/10.5281/zenodo.3878122>, 2019
- 368 Hersbach, H., Bell, B., Berrisford, P., Hirahara, S., Horányi, A., Muñoz-Sabater, J., Nicolas, J., Peubey, C., Radu, R.,
369 Schepers, D., Simmons, A., Soci, C., Abdalla, S., Abellan, X., Balsamo, G., Bechtold, P., Biavati, G., Bidlot, J., Bonavita,
370 M., De Chiara, G., Dahlgren, P., Dee, D., Diamantakis, M., Dragani, R., Flemming, J., Forbes, R., Fuentes, M., Geer, A.,
371 Haimberger, L., Healy, S., Hogan, R.J., Hólm, E., Janisková, M., Keeley, S., Laloyaux, P., Lopez, P., Lupu, C., Radnoti, G.,
372 de Rosnay, P., Rozum, I., Vamborg, F., Villaume, S., Thépaut, J.-N.: Complete ERA5 from 1950: Fifth generation of
373 ECMWF atmospheric reanalyses of the global climate. Copernicus Climate Change Service (C3S) Data Store (CDS), 2023
- 374 Hersbach, H., Bell, B., Berrisford, P., Hirahara, S., Horányi, A., Muñoz-Sabater, J., Nicolas, J., Peubey, C., Radu, R.,
375 Schepers, D., Simmons, A., Soci, C., Abdalla, S., Abellan, X., Balsamo, G., Bechtold, P., Biavati, G., Bidlot, J., Bonavita,
376 M., De Chiara, G., Dahlgren, P., Dee, D., Diamantakis, M., Dragani, R., Flemming, J., Forbes, R., Fuentes, M., Geer, A.,
377 Haimberger, L., Healy, S., Hogan, R.J., Hólm, E., Janisková, M., Keeley, S., Laloyaux, P., Lopez, P., Lupu, C., Radnoti, G.,
378 de Rosnay, P., Rozum, I., Vamborg, F., Villaume S., Thépaut, J.-N.: The ERA5 global reanalysis. *Q. J. R. Meteorol. Soc.*,
379 146, 1999–2049, <https://doi.org/10.1002/qj.3803>, 2020
- 380 ICES Bottle and low-resolution CTD dataset, Extractions 22 DEC 2013 (for years 1990–20012), 25 FEB 2015 (for year
381 2013), 13 OCT 2016 (for year 2015), 15 JAN 2019 (for years 2016–2017), 22 SEP 2020 (for year 2018), 10 MAR 2021 (for
382 years 2019–202), 28 FEB 2022 (for year 2021), ICES, Copenhagen, 2022
- 383 IPCC: Climate Change 2021: The Physical Science Basis. Working Group I Contribution to the IPCC Sixth Assessment
384 Report. doi:10.1017/9781009157896, 2021
- 385 Kniebusch, M., Meier, H. E. M., Radtke, H.: Changing salinity gradients in the Baltic Sea as a consequence of altered
386 freshwater budgets. *Geophys. Res. Lett.*, 46, 9739–9747, <https://doi.org/10.1029/2019GL083902>, 2019
- 387 Lehmann, A., Myrberg, K., Post, P., Chubarenko, I., Dailidiene, I., Hinrichsen, H.-H., Hüsey, K., Liblik, T., Meier, H. E. M.,
388 Lips, U., Bukanova, T.: Salinity dynamics of the Baltic Sea. *Earth Syst. Dynam.*, 13(1), 373–392,
389 <https://doi.org/10.5194/esd-13-373-2022>, 2022



- 390 Leppäranta, M., Myrberg, K.: Physical Oceanography of the Baltic Sea. Springer-Verlag, 378 pp., ISBN 978-3-540-79702-9,
391 2009
- 392 Lindenthal, A., Hinrichs, C., Jandt-Scheelke, S., Kruschke, T., Lagemaat, P., van der Lee, E. M., Morrison, H. E., Panteleit, T.
393 R., Raudsepp, U.: Baltic Sea Surface Temperature Analysis 2022: A Study of Marine Heatwaves and Overall High Seasonal
394 Temperatures. State of the Planet Discussions, <https://doi.org/10.5194/sp-2023-23>, 2023
- 395 Lindstrom, E., Gunn, J., Fischer, A., McCurdy, A., Glover, L. K.: A Framework for Ocean Observing. Task Team for an
396 Integrated Framework for Sustained Ocean Observing, <https://doi.org/10.5270/OceanObs09-FOO>, 2012
- 397 Lu, Y., Li, Y., Lin, P., Duan, J., Wang, F.: North Atlantic–Pacific salinity contrast enhanced by wind and ocean warming. Nat.
398 Clim. Chang., 14(7), 723–731, <https://doi.org/10.1038/s41558-024-02033-y>, 2024
- 399 McGrath, M., Poynting, M., Rowlatt, J.: Climate change: World's oceans suffer from record-breaking year of heat. BBC
400 News Climate & Science, Retrieved from <https://www.bbc.com/news/science-environment-68921215>, 2024
- 401 Meier, H. E. M., Kauker, F.: Modeling decadal variability of the Baltic Sea: 2. Role of freshwater inflow and large-scale
402 atmospheric circulation for salinity. J. Geophys. Res., 108, 3368, <https://doi.org/10.1029/2003JC001799>, 2003
- 403 Meier, H. E. M., Dieterich, C., Gröger, M., Dutheil, C., Börgel, F., Safonova, K., Christensen, O. B., Kjellström, E.:
404 Oceanographic regional climate projections for the Baltic Sea until 2100. Earth Syst. Dynam., 13, 159–199,
405 <https://doi.org/10.5194/esd-13-159-2022>, 2022
- 406 Meyssignac, B., Boyer, T., Zhao, Z., Hakuba, M.Z., Landerer, F.W., Stammer, D., Köhl, A., Kato, S., L'ecuyer, T., Ablain,
407 M., Abraham, J.P.: Measuring global ocean heat content to estimate the Earth energy imbalance. Front. Mar. Sci., 6, 432,
408 <https://doi.org/10.3389/fmars.2019.00432>, 2019
- 409 Mohrholz, V.: Major Baltic inflow statistics–revised. Front. Mar. Sci., 5, 384, <https://doi.org/10.3389/fmars.2018.00384>,
410 2018
- 411 Nontapa, C., Kesamoon, C., Kaewhawong, N., Intrapai boon, P.: A New Time Series Forecasting Using Decomposition
412 Method with SARIMAX Model. In: Yang, H., Pasupa, K., Leung, A.C.S., Kwok, J.T., Chan, J.H., King, I. (eds). Neural
413 Information Processing. Commun. Comput. Inf. Sci., vol 1333, Springer, Cham,
414 https://doi.org/10.1007/978-3-030-63823-8_84, 2020
- 415 Panteleit, T., Verjovkina, S., Jandt-Scheelke, S., Spruch, L., Huess, V.: EU Copernicus Marine Service Quality Information
416 Document for the Baltic Sea Physics Reanalysis Product. Mercator Ocean International,
417 <https://catalogue.marine.copernicus.eu/documents/QUID/CMEMS-BAL-QUID-003-011.pdf>, last access: 12 April 2023
- 418 Radtke, H., Brunnabend, S.-E., Gräwe, U., Meier, H. E. M.: Investigating interdecadal salinity changes in the Baltic Sea in a
419 1850–2008 hindcast simulation. Clim. Past, 16, 1617–1642, <https://doi.org/10.5194/cp-16-1617-2020>, 2020
- 420 Ranasinghe, R., Ruane, A.C., Vautard, R., Arnell, N., Coppola, E., Cruz, F.A., Dessai, S., Islam, A.S., Rahimi, M., Ruiz
421 Carrascal, D., Sillmann, J., Sylla, M.B., Tebaldi, C., Wang, W., Zaaboul, R.: Climate Change Information for Regional
422 Impact and for Risk Assessment. In: Masson-Delmotte, V., Zhai, P., Pirani, A., Connors, S.L., Péan, C., Berger, S., et al.
423 (eds.). Climate Change 2021: The Physical Science Basis. Working Group I Contribution to the IPCC Sixth Assessment
424 Report. Cambridge University Press, <https://doi.org/10.1017/9781009157896.014>, 2021
- 425 Raudsepp, U., Maljutenko, I.: A method for assessment of the general circulation model quality using K-means clustering
426 algorithm: A case study with GETM v2.5. Geosci. Model Dev., 15, 535–551, <https://doi.org/10.5194/gmd-15-535-2022>,
427 2022



- 428 Raudsepp, U., Maljutenko, I., Barzandeh, A., Uiboupin, R., and Lagema, P.: Baltic Sea freshwater content, in: 7th edition of
429 the Copernicus Ocean State Report (OSR7), edited by: von Schuckmann, K., Moreira, L., Le Traon, P.-Y., Grégoire, M.,
430 Marcos, M., Staneva, J., Brasseur, P., Garric, G., Lionello, P., Karstensen, J., and Neukermans, G., Copernicus Publications,
431 State Planet, 1-osr7, 7, <https://doi.org/10.5194/sp-1-osr7-7-2023>, 2023.
- 432 Raudsepp, U., Maljutenko, I., Haapala, J., Männik, A., Verjovkina, S., Uiboupin, R., von Schuckmann, K., Mayer, M.:
433 Record high heat content and low ice extent in the Baltic Sea during winter 2019/20. In: Copernicus Ocean State Report,
434 Issue 6, Journal of Operational Oceanography, 15:sup1, s175–s185; DOI:10.1080/1755876X.2022.2095169, 2022.
- 435 Ringgaard, I., Korabel, V., Spruch, L., Lindenthal, A., Huess, V.: EU Copernicus Marine Service Product User Manual for
436 the Baltic Sea Physics Reanalysis Product. Mercator Ocean International,
437 https://catalogue.marine.copernicus.eu/documents/PUM/CMEMS-BAL-PUM-003-011_012.pdf, last access: 1 July 2024
- 438 Schubert, S.D., Chang, Y., DeAngelis, A.M., Koster, R.D., Lim, Y.-K., Wang, H.: Exceptional Warmth in the Northern
439 Hemisphere during January–March of 2020: The Roles of Unforced and Forced Modes of Atmospheric Variability. *J. Clim.*,
440 35(8), 2565–2584, <https://doi.org/10.1175/JCLI-D-21-0291.1>, 2022
- 441 Safonova, K., Meier, H.E.M., Gröger, M.: Summer heatwaves on the Baltic Sea seabed contribute to oxygen deficiency in
442 shallow areas. *Commun. Earth Environ.*, 5, 106, <https://doi.org/10.1038/s43247-024-01268-z>, 2024
- 443 Savchuk, P.: Large-Scale Nutrient Dynamics in the Baltic Sea, 1970–2016. *Front. Mar. Sci.*, 5, 95,
444 <https://doi.org/10.3389/fmars.2018.00095>, 2018
- 445 Skliris, N., Marsh, R., Josey, S.A., Good, S.A., Liu, C., Allan, R.P.: Salinity changes in the World Ocean since 1950 in
446 relation to changing surface freshwater fluxes. *Clim. Dyn.*, 43(3-4), 709–736, <https://doi.org/10.1007/s00382-014-2131-7>,
447 2014
- 448 Uotila, P., Vihma, T., Haapala, J.: Atmospheric and oceanic conditions and the extremely low Bothnian Bay sea ice extent in
449 2014/2015. *Geophys. Res. Lett.*, 42, 7740–7749, <https://doi.org/10.1002/2015GL064901>, 2015